

A Reconfigurable Image Tube using an External Electronic Image Readout

J.S. Lapington^{*1}, J. Howorth² and J. Milnes²

¹ Space Research Centre, University of Leicester, University Road, Leicester, LE1 7RH, U.K.

² Photek Ltd, 26 Castleham Road, St. Leonards on Sea, East Sussex, TN38 9NS, U.K.

ABSTRACT

We have designed and built a sealed tube microchannel plate (MCP) intensifier for optical/NUV photon counting applications suitable for 18, 25 and 40 mm diameter formats. The intensifier uses an electronic image readout to provide direct conversion of event position into electronic signals, without the drawbacks associated with phosphor screens and subsequent optical detection. The Image Charge technique is used to remove the readout from the intensifier vacuum enclosure, obviating the requirement for additional electrical vacuum feedthroughs and for the readout pattern to be UHV compatible. The charge signal from an MCP intensifier is capacitively coupled via a thin dielectric vacuum window to the electronic image readout, which is external to the sealed intensifier tube. The readout pattern is a separate item held in proximity to the dielectric window and can be easily detached, making the system easily reconfigurable. Since the readout pattern detects induced charge and is external to the tube, it can be constructed as a multilayer, eliminating the requirement for narrow insulator gaps and allowing it to be constructed using standard PCB manufacturing tolerances. We describe two readout patterns, the tetra wedge anode (TWA), an optimized 4 electrode device similar to the wedge and strip anode (WSA) but with a factor 2 improvement in resolution, and an 8 channel high speed 50 ohm device, both manufactured as multilayer PCBs. We present results of the detector imaging performance, image resolution, linearity and stability, and discuss the development of an integrated readout and electronics device based on these designs.

Keywords: Microchannel plate, MCP, image intensifier, Image Charge, PCB, ASIC, integrated readout

1. INTRODUCTION

Despite the recent development of low light level CCDs¹ with in-built charge gain functionality, the microchannel plate (MCP) based intensifier still has an important role for optical applications where low noise, single photon counting is required, and is the only option where a combination of high resolution imaging with high precision photon timing is required. Imaging MCP based intensifiers are available in two fundamental forms; those comprising an optical intensifier optically coupled to a solid state optical sensor, as typified by the intensified CCD², and those utilising direct electronic sensing of the charge produced by the MCP itself, after amplification of the single photoelectron per event.

Electronic sensing has traditionally meant either detection with an active device, such as a CCD in an electron bombarded CCD (EBCCD)³, or with a passive device such as a resistive anode position readout⁴. The advantages of the EBCCD include the ubiquitous nature of CCD devices with their fixed pixel structure and TV scan readout, and the inherent gain produced by energy conversion process of accelerated MCP produced electrons in silicon (3.6 eV per electron hole pair). Their physical disadvantages include the vacuum incompatibility and degradation under high energy electron bombardment of the CCD itself, and the practical issues of manufacturing an ultra high vacuum (UHV) enclosure containing a CCD with reliable vacuum electrical feedthroughs. In terms of performance, they offer limited advantages over normal intensified CCDs, since quantum efficiency (QE) is still dominated by the photocathode response (typically <25%), and their time resolution is limited by the frame readout nature of all CCDs.

* jon@lapington.com; phone +44 116 2523498; fax +44 116 2522464; src.le.ac.uk

Traditionally, passive electronic imaging devices which simply collect the MCP output charge among a number of electrodes, such as the resistive anode whereby charge is collected and divided by a resistive sheet, or a conductive device such as the wedge and strip anode (WSA)⁵, which rely on geometrical charge division, suffer some of the same limitations as the EBCCD. Since the imaging component is contained within the intensifier vacuum enclosure they must be UHV compatible and require a number of additional electrical vacuum feedthroughs to interface with the outside world.

In this paper we describe a prototype intensifier tube which utilizes the Image Charge⁶ technique to decouple an electronic image readout device from the intensifier tube (see figure 1). Image Charge functions by collecting the output MCP event charge on an anode comprising a two dimensional resistive sheet within the vacuum enclosure. The resistive sheet, served by a single electrical connection around its perimeter, serves only to localize the event charge during the timescale of its electronic measurement. The localized charge induces a signal through the dielectric substrate on which the resistive layer is deposited and which acts as the rear surface of the intensifier vacuum enclosure, to the electronic position readout device held in proximity to the rear face of the substrate. This technique is suitable for any conductive readout device requiring an extended charge footprint, and provides numerous benefits including simplicity of manufacture, practical operational, imaging performance and configuration flexibility advantages.

The WSA is a conductive readout device which benefits greatly from combination with the Image Charge technique. The WSA typifies the family of conductive charge division readouts using geometrical charge division by means of a patterned planar array of isolated conductors. While such devices have an underlying simplicity in design and implementation, requiring only a small number of charge measurement channels (three in the case of the WSA), in practice, when used in the mode where charge is directly collected on the electrodes, their performance is compromised by physical processes which distort the collected charge ratios. These distortions depend on the event count rate and distribution of illumination, and give rise to time dependent image shifts and nonlinearities. These limitations have been thoroughly discussed and methods described to limit their effect elsewhere⁷. However, when used with Image Charge, WSA performance is enhanced. Not only does the charge induction technique eliminate rate and image dependent charge ratio distortions, but partition noise, a statistical noise resulting from the collection of quantized electronic charge, is also absent.

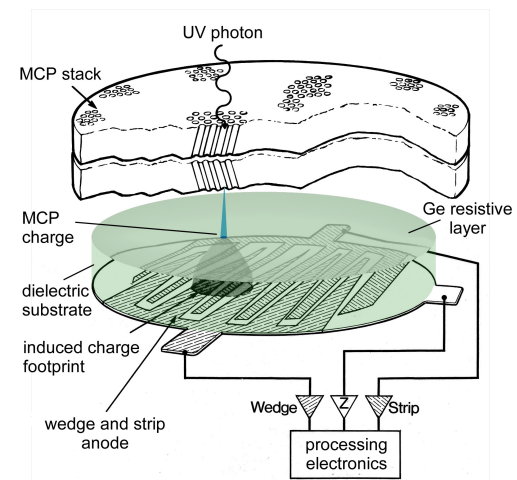


Figure 1. A schematic of Image Charge using an MCP stack with a wedge and strip image readout.

We have maximised the benefits of using conductive charge division patterns with Image Charge by developing new readout pattern designs, one of which is called the tetra wedge anode (TWA)⁸. The TWA takes advantage of the through-substrate charge induction technique utilized by Image Charge, by making use of multi-layer printed circuit board (PCB) technology to greatly relax the pattern manufacturing constraints, simplify manufacture, and allow a two-fold performance enhancement over the traditional WSA by maximization of the electrode dynamic range.

While the enhanced performance of the TWA charge division pattern offers high performance resolution ($> 1000 \times 1000 \text{ pixel}^2$), it is fundamentally a serial event processing device, and its ultimate count rate, ignoring any count rate limitations caused by local event saturation effects in the MCP stack, is limited by the event processing time, itself constrained by the requirement to achieve a given electronic signal to noise ratio necessary for the chosen position resolution. For applications where very high count rates or very high time resolution is required, a different approach to pattern design has to be made. We have developed a number of readout devices optimised for very high speed operation with the Image Charge technique. These devices utilize an array of parallel electrodes, each configured with a matching ground plane as a 50Ω microstrip. While the initial devices give only one dimensional imaging and are low in channel number (currently 8 channels) this configuration is capable of simultaneous parallel channel readout at very high speed, due to the optimised 50Ω transmission line which minimizes signal dispersion. In conjunction with small pore MCPs,

which can produce event pulses with a width of a few hundred picoseconds, this will enable a detector event timing resolution of the order of a few tens of picoseconds to be reliably achieved. Not only can the TWA and $50\ \Omega$ high speed readout be used with the same generic Image Charge intensifier tube, but the flexibility offered by this technique, due to the complete mechanical and electronic decoupling provided by charge induction, allows the readouts to be hot swapped while in operation.

The next stage in readout development, which has already been initiated, is the integration of the electronics on to the readout substrate. Miniaturization of the readout electronics by the use of multi-channel application specific integrated circuit (ASIC) front end devices will allow high channel counts to be achieved on a relatively small footprint, the entire front end electronics being optimally situated on the under side of the readout substrate, directly adjacent to the readout electrodes themselves. A multi chip module PCB substrate will be used as the platform to integrate the readout pattern and wire bonded ASIC dies. Associated FPGA based digital control electronics will reside on an adjacent board, interfacing with the outside world via a generic interface such as USB 2.0 or Firewire, IEEE 1394.

Several possible ASIC solution already exist, the most promising of these, especially for very high speed operation with high event time resolution, being the NINO⁹ ASIC, an ultra fast front-end preamplifier-discriminator chip developed for the precision time measurement required for the ALICE Time-Of-Flight detector, one of the experiments planned for the CERN Large Hadron Collider (LHC). The current version of the chip has 8 channels with a peaking time of 1ns with a time resolution of 20ps rms.

2. DESIGN AND OPERATION

2.1 Detector design

The Image Charge detector design is based on a well proven Photek commercial product using a chevron stack of 25 mm microchannel plates. A schematic of the design is shown in figure 2. The upper half of the detector uses a standard intensifier design with and optical photocathode proximity focussed to the MCP input, supported on an optical window. The intensifier will use $3\ \mu\text{m}$ pore diameter MCPs manufactured by Photonis, which have only recently become available commercially. The small geometry of the $3\ \mu\text{m}$ pore MCPs allows the MCP gain process, an electron avalanche, to propagate very quickly; pulse rise-time and width being directly dependent on MCP pore size. These MCPs produce extremely narrow pulse widths and enable the best possible time resolution to be achieved. Recent experiments demonstrate a pulse rise-time and length of 80 ps and 140 ps respectively (see figure 3) from a 2 MCP stack in a photon counting configuration.

The output of the intensifier incorporates an Image Charge interface, replacing the standard phosphor screen with a planar “resistive sea” which serves to localize the event charge while the induced event signal is detected on the image readout.

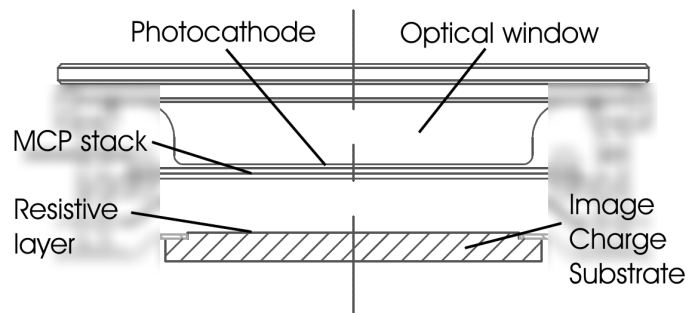


Figure 2. A schematic of Image Charge intensifier, shown in cross section, showing the optical window, photocathode, MCP stack, Image charge resistive layer, and substrate.

Commercially sensitive design elements are blurred out.

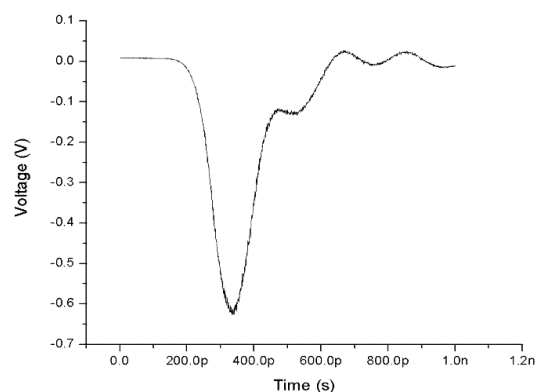


Figure 3. A plot of the pulse shape from a 2 stage MCP detector with $3\ \mu\text{m}$ pores representing a risetime of 80 ps.

2.2 Image Charge

The already proven Image Charge technique, shown in figure 1, is crucial to this device, serving to isolate the readout from the detector and providing several operational and practical benefits. Redistribution of secondary electrons produced when the event charge is collected on the readout anode imposes major performance limitations on traditional electronic readout devices⁷. Image Charge overcomes these limitations, improving image linearity, resolution and stability. The simple dielectric interface between detector and readout offers operational flexibility and electrical and vacuum isolation. The readout is mechanically separate from the detector, and thus a generic intensifier of simple design capable of operating with a variety of readouts for different applications, can be used. The readout can be manufactured using PCB techniques without the vacuum compatibility, cleanliness and electrical feedthrough issues associated with direct charge collection inside the detector enclosure.

2.3 TWA high resolution readout

The TWA was originally conceived of as a planar four electrode device, whose novel geometry allows the theoretical dynamic range of the pairs of electrodes used to encode each axis to vary from 0% to 100%, unlike the WSA, which is limited theoretically from between 0% to 50%. In practice, constraints imposed by manufacturing limitations and interelectrode capacitance considerations which force non zero minimum electrode widths and interelectrode insulating gaps, cause the theoretical dynamic range in both cases to be reduced by $\sim 1/3$. However this still leaves the TWA with a factor 2 advantage in imaging performance over the WSA. This advantage can either be utilized to increase image resolution, or to decrease the pulse processing time for a given signal to noise ratio and hence increase the maximum event rate for a given image resolution.

In its original planar conception, the TWA comprised two electrodes resembling interlocking combs with a typical pitch of 1-2 mm, together with two interposed electrodes in the form of zigzags. The zigzag electrodes limited the geometrical optimization of the pattern due to their individual occurrence twice within each pitch and their end to end resistance. However, since electrode material does not need to be exposed for the collection of signal charge when using the Image Charge technique, the electrodes can be constructed on two layers of a multi-layer PCB, with adjacent electrodes arranged to be on alternate layers, avoiding limitations imposed by minimum interelectrode gaps. In this arrangement the TWA pattern can be organized as two pairs of interlocking comb-like electrodes, with each electrode occurring only once in every pattern pitch, eliminating the requirement for zigzag shaped electrodes with potentially high resistance. The smallest practical separation of 100 μm was used between the two PCB layers defining the pattern electrodes, in order to achieve as close to 50:50 charge sharing as possible. A schematic of the two layer Image Charge TWA is shown in figure 4.

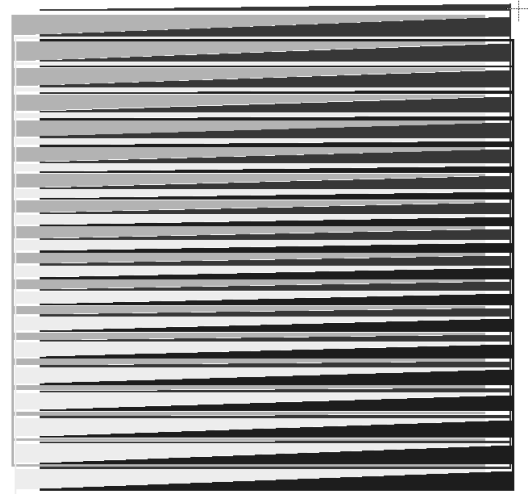


Figure 4. A schematic of the TWA design optimised for use with Image Charge, consisting of 2 pairs of interlocking combs.

2.4 50 Ω high speed readout

Though the performance benefits of Image Charge had already been proven very successfully using a traditional planar WSA readout¹⁰, there had been concerns in some quarters that the resistive anode would impact the propagation of the event signal to the readout electrodes, despite the purely capacitive signal coupling. So a simple 8 electrode high speed readout was designed and manufactured to assess the speed potential of the Image Charge technique. This device consisted of eight 50 Ω microstrip electrodes spaced at a pitch of 2 mm. A modified microstrip design was chosen with the ground plane electrode equal in width to the sense electrode in order to prevent event signal pick-up on the ground plane with resultant signal attenuation. Two different microstrip geometries were used though the pitch between microstrips was kept constant.

The two modified microstrip designs used thin and thick microstrip widths of 0.15 mm and 1.0 mm respectively, and sense to ground electrode separations of 0.09 mm and 0.6 mm respectively. The two designs were used to assess the trade-offs between the levels of event signal coupling (driven by the microstrip widths), the sensitivity to variations in the external surrounding dielectrics (the thin width/separation microstrip being less sensitive), and the effects of crosstalk between microstrips (the thick width microstrip being more sensitive).

Both microstrip anode designs were manufactured on a custom multi-layer PCB using FR4 prepreg and laminate. The precise dimensions of the microstrips were calculated by using a two dimensional finite element analysis (FEA) simulation to determine the capacitance between microstrips, assuming infinite length microstrips i.e. a constant cross-section in the third dimension. The Image Charge substrate and the exact geometry of the PCB (e.g. dielectric constants, electrode thicknesses and embedded electrodes) were included in this model and the geometry iterated to produce a nominal $50 \Omega \pm 10\%$ impedance, calculated using the relationship :-

$$Z_0 = \frac{1}{c\sqrt{CC_0}}, \quad (1)$$

where Z_0 is the microstrip impedance, C is the microstrip capacitance per metre, and C_0 is similar but with all dielectrics set to $\epsilon_r = 1$, and c is $3 \times 10^8 \text{ ms}^{-2}$.

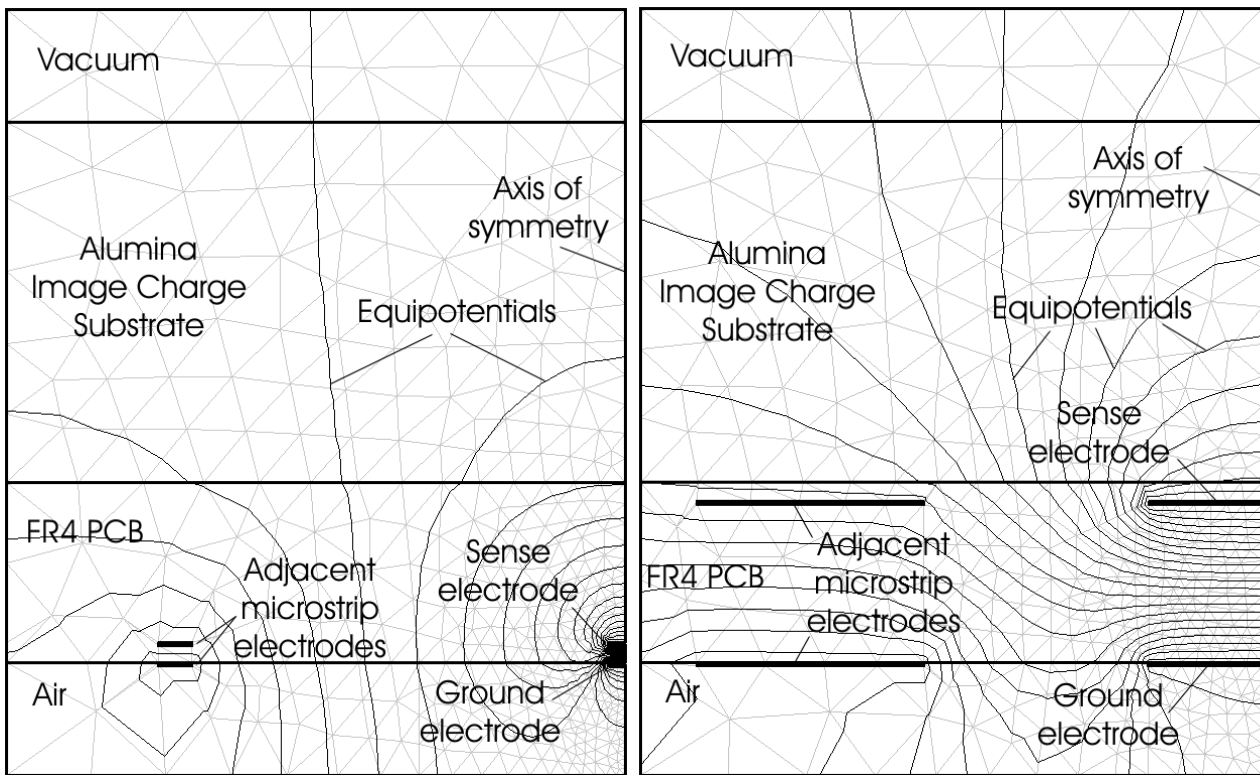


Figure 5. Finite element analysis electrostatic field simulations used to calculate microstrip dimensions for the thin and thick electrode designs respectively. The diagrams show the cross-section geometry, substrate material, equipotentials and FEA elements used in the simulation.

3. RESULTS

3.1 TWA performance

In Image Charge mode, the image resolution of the TWA is solely as a result of electronic noise, there being no contribution from partition noise since the charge quanta are not discretely divided among the individual electrodes.

Initial imaging studies were carried out using a traditional planar 33 mm diameter WSA manufactured using copper electrodes on a quartz substrate and optimized for low capacitance, and hence low electronic noise. Comparison of the noise performance of a simulated event using a reference pulser indicated the noise contributions at an equal gain of 2.6×10^7 electrons, to be 47 μm FWHM for the WSA, but only 15 μm FWHM for the TWA. This is even larger than the expected twofold improvement, and resulted from the WSA being designed for direct charge collection and having a smaller pitch to avoid image modulation; the pitch was 890 μm for the WSA as opposed to 1280 μm for the TWA.

This result illuminates another benefit of the Image Charge technique: controlled charge footprint spread within the dielectric. In a traditional WSA detector in which charge is directly collected by the WSA, a relatively large MCP to WSA gap is required to allow the charge exiting the MCP to spread sufficiently to eliminate image modulation, an effect whereby the charge footprint is too small to average out the fine repetitive structure of the readout pattern. The large gap requires an extended vacuum enclosure and field rings to define a uniform field region within the gap, increasing the mechanical and electrical complexity together with the detector size. In addition, this physical charge spread is prone to distortion (and thus image nonlinearity) resulting from field non-uniformity, especially near the perimeter of the imaging area near the MCP exit face, due to intrusion of the lower MCP mechanical support in a region where the output electrons have the lowest energy.

In comparison, in an Image Charge detector, the MCP output charge can be proximity focussed to the Image Charge resistive layer, virtually eliminating any scope for spatial distortion at this interface. The mechanism for charge induction via capacitive coupling between the localized event charge on the resistive layer and the readout electrodes causes the induced charge footprint to be spread in a very well defined manner, with a radial charge distribution described by the equation :-

$$\sigma_r \propto \frac{1}{(r^2 + a^2)^{3/2}} \quad (2)$$

where σ_r is the induced charge at horizontal radius r , across a dielectric of thickness a . This equation describes the charge induced from a point charge on a continuous conductive plane at a distance, a ; a close approximation to the pattern geometry which has a subdivided electrode plane.

In terms of the electronics, the four channel TWA is a direct replacement for the resistive disk anode used in the existing Photek IPD detectors, and uses the same four channel electronics and an identical image encoding algorithm. Even with identical electronics, the TWA benefits from decreased electronic noise compared with the resistive anode due to the lack of resistive coupling between amplifiers, the potential to use high value bias resistors owing to the net zero signal current flow in Image Charge mode, and the reduction in interelectrode capacitance possible with the Image Charge because a larger pattern pitch can be utilized. The net result in terms of position resolution is an improvement of a factor two over the WSA, and a factor four or greater over the resistive anode. Image resolution and linearity of the TWA was measured using a pinhole mask with a hole size of 50 μm and centre to centre spacing of 0.5 mm. Figure 6a shows an image of the 25 mm active area of the detector illuminated through the pinhole mask. Pincushion distortion near the edge of the field of view is a feature of the demountable detector used for this experiment and results from electrostatic distortion in the region between the MCP to Image Charge resistive layer, caused by intrusion of the thick MCP mount. A zoomed area of the centre of the field of view is shown in figure 6b. The measured resolution from this data is 62 μm FWHM at a gain of 1.5×10^7 electrons. After deconvolution of the pinhole mask, this represents an intrinsic detector resolution of 36 μm FWHM. The electronic noise measurement, made using a pulse generator with the pattern attached to the electronics, is 15 μm FWHM at a gain of 2.6×10^7 electrons, which equates to 26 μm FWHM when extrapolated to the TWA operating gain.

Three TWA patterns were designed with varying pattern pitch and perimeter contact geometries to assess the optimum pattern parameters. Since the pincushion distortion resulting from the rear detector geometry dominates the nonlinearity, it is not possible to separate the effect due to the pattern design alone. In parallel with this, a software simulation using the pattern design including the exact perimeter contact geometry was used in, conjunction with the radial induced charge distribution from equation 2, to simulate the image linearity. Figure 7 shows simulation of the original pattern used for the imaging experiments described here compared to the latest design currently under manufacture, indicating the dramatic the improvement in linearity.

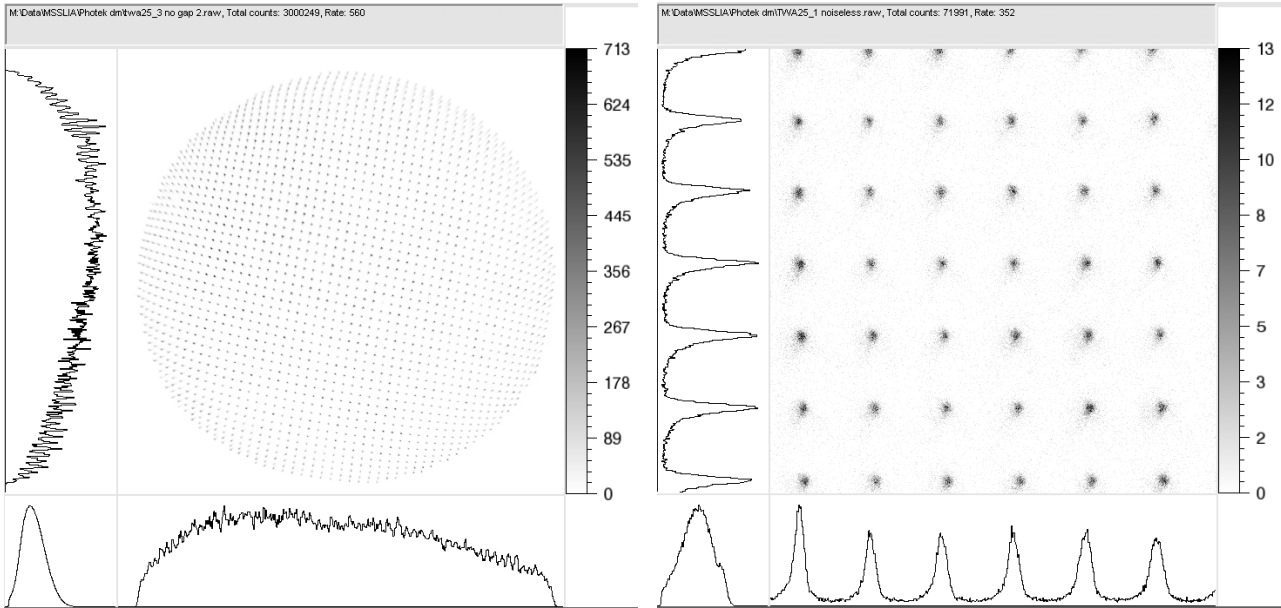


Figure 6. Figure 6a shows the image of the detector field of view using an Image Charge TWA, illuminated through a pinhole mask with $50\ \mu\text{m}$ pinholes at a spacing of $0.5\ \text{mm}$. Figure 6b shows a zoomed portion of a TWA image illuminated via the same mask but using another of the TWA designs. The data equates to a TWA resolution of $36\ \mu\text{m}$ FWHM at a gain of 1.5×10^7 electrons after pinhole deconvolution and was taken at a count rate of $22\text{k}\ \text{ct}\ \text{s}^{-1}$.

The secondary electrons produced during the collection of primary electrons from an MCP on a readout anode⁷ can pose significant problems for devices employing conductive charge division since they are able to mediate charge redistribution. Secondary electron redistribution is driven by small interelectrode voltages, generated across the electrode DC bias resistors by signal currents, which are image and count rate dependent. Readouts which directly collect charge can thus exhibit count rate and image distribution dependent spatial distortions. In contrast, secondary electron production in an Image Charge detector will merely redistribute the charge distribution on the resistive anode

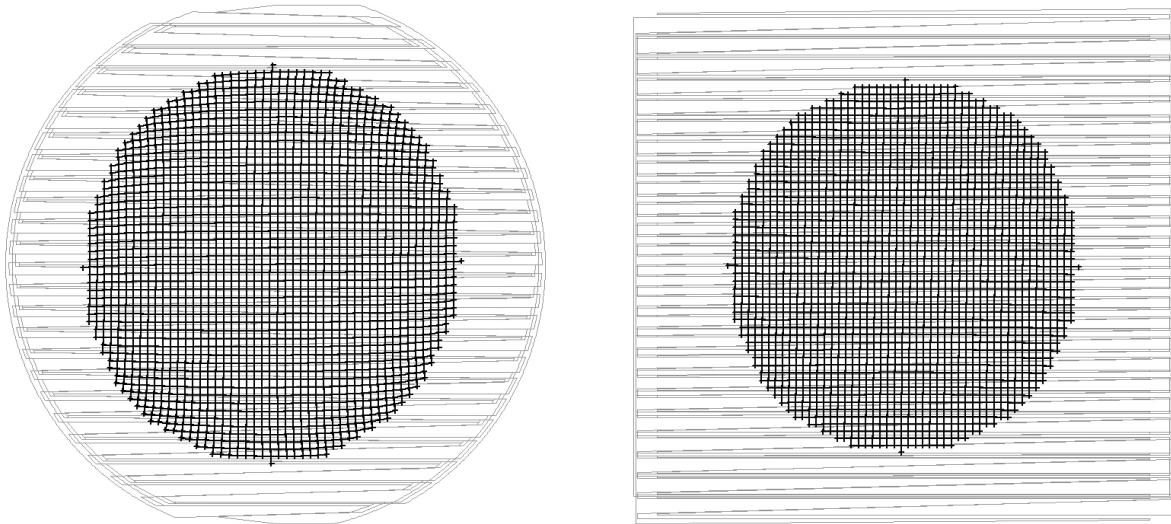


Figure 7. Simulations of the predicted linearity for a regular array over the detector field of view on the current TWA design (left) compared with the latest design (right) currently under manufacture. The pattern design is shown in the background

layer, maintaining the symmetry of the distribution and centroid position, and thus does not give rise to position shifts. This is borne out by results from the position resolution measurements which indicated that the position error of the mean coordinates of the nine pinholes used to measure the resolution had a standard deviation of $11.0\ \mu\text{m}$ and $12.8\ \mu\text{m}$ in the x and y axes respectively, over a detector count rate range of $5\text{k}\ \text{ct}\ \text{s}^{-1}$ to $200\text{k}\ \text{ct}\ \text{s}^{-1}$, less than the position resolution of the detector.

The dominant factor limiting the count rate capability of the Image Charge detector is pulse pile-up in the charge measurement electronics. The shaping amplifiers use a $0.5\ \mu\text{s}$ shaping time and are designed to minimize signal deadtime for a given signal to noise ratio by use of a complex pole pair shaping scheme which provides very fast return to baseline performance compared to standard C-R shaping networks. The count rate capability of the TWA has not yet been measured but is expected to match the performance of the Image Charge WSA detector, shown in figure 8, which was obtained using 3 channels of the same electronics.

3.2 8 electrode $50\ \Omega$ microstrip

The 8 electrode $50\ \Omega$ microstrip readout has only just begun preliminary testing. The success of the calculations in providing a $50\ \Omega$ impedance along the entire length of each electrode was measured using time domain reflectometry. The thick electrode version (1 mm wide electrodes) achieved $58\ \Omega$, however the thin electrode version of the pattern was not as successful, being $73\ \Omega$ along its length. The error in the latter is probably due in part to the limitations of the FEA electrostatic simulation. The software was limited to a restricted number of elements, a factor which would have had greater impact on the smaller geometry of the thin electrode pattern. Another error factor was the geometric accuracy required of the laminate thickness, which was more demanding for the thin electrode design; the narrow electrode separation being highly sensitive to a small variation in laminate thickness.

We have very recently manufactured a sealed tube Image Charge intensifier using a stack of 2 MCP with $7\ \mu\text{m}$ pores.

Figure 9 shows the time response measured from a single electrode of the pattern attached to this intensifier, using a 5 GHz oscilloscope. The risetime of the pulse is $\sim 200\ \text{ps}$ is entirely consistent with the $7\ \mu\text{m}$ pore MCPs, though it may be limited by the bandwidth of the oscilloscope. In addition, the $50\ \Omega$ electrode was not terminated and so reflections from the open end will confuse the signal, and the other readout channels were not populated. Even so, this is a promising first result and we expect the final device using $3\ \mu\text{m}$ pore MCPs to closely reflect the single channel pulse speed shown in figure 3.

3.3 Operational flexibility

Having battled previously manufacturing and operating sealed tube intensifiers with a variety of internal electronic readouts, including WSAs, Spiral Anodes, and delay lines, the ease of operation of an Image Charge device comes as a great relief. No longer does the readout device have to meet the strictures of UHV compatibility, have to withstand bakeout temperatures, or require mechanical housing within the vacuum enclosure with provision of multiple electronic

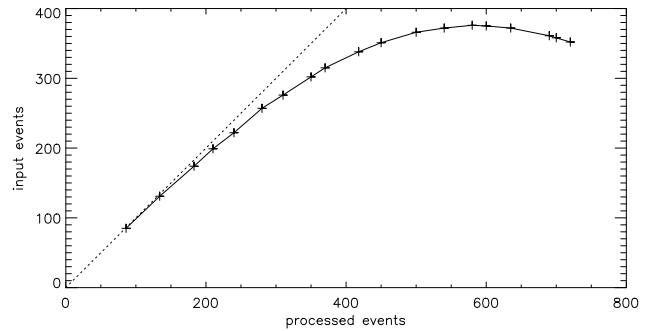


Figure 8. The count rate performance in kiloevents per second of an Image Charge WSA using Photek $0.5\ \mu\text{s}$ pulse shaping electronics.

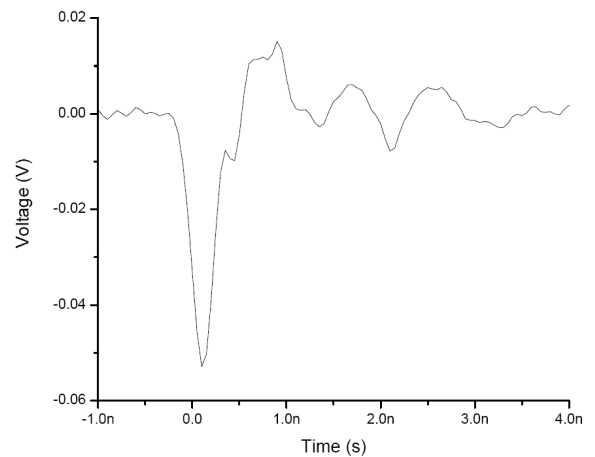


Figure 9. A plot of the pulse shape from one channel of the 8 electrode $50\ \Omega$ readout using a $7\ \mu\text{m}$ pore double MCP detector, and representing a risetime of $\sim 200\ \text{ps}$.

vacuum feedthroughs. If the Image Charge readout device fails, it is extremely straightforward to replace; certainly not the case with an internal readout device after manufacture of the tube.

The first tests of the TWA were made using a very simple mechanical mount to hold it in-situ against the Image Charge tube, though in fact the high resolution of the TWA identified this as a limitation; the image could be seen to gradually creep owing to spring of the signal cables. As soon as the method of mounting the TWA was improved the problem was cured, and the readout could still be released from the detector in around 5 seconds! This description accurately characterizes the simplicity of electronic readout operation using an Image Charge tube.

The other great benefit of the Image Charge technique is that the tube is now a generic design, which can remain in-situ while the image readout is changed. This opens the possibility of a modular, reconfigurable detector capable of a variety of modes of operation, which can be changed very rapidly. For example, the detector could be switched from having a very high count rate, high time resolution with simultaneous detection capability, to a very high spatial resolution capability in a matter of seconds.

4. CONCLUSIONS

We have demonstrated that a detector based on a sealed tube MCP intensifier employing an Image Charge coupled position readout is a highly versatile device. The generic Image Charge intensifier tube can be manufactured using the latest small pore, high performance microchannel plates to provide high time resolution combined with their potential for very high position resolution. We have shown that the Image Charge technique of coupling a position readout to an intensifier tube is compatible with a range of readouts optimised for high spatial and high temporal resolution, and the ease with which the readout can be reconfigured provides a large degree of operational flexibility. The Image Charge intensifier is a much more practical proposition, in a commercial context, to exploit the benefits of a large variety of electronic readout devices, being much simpler to manufacture and operate. It does not require the inclusion of the position readout within the UHV intensifier enclosure, with its associated manufacturing and technological difficulties. This enables the position readout to be manufactured using PCB techniques without the vacuum compatibility, cleanliness and electrical feedthrough issues associated with direct charge collection inside the detector enclosure. The position readout is mechanically and electrical independent and can even be hot-swapped.

These features lend this technique to the next generation of readout devices, comprising the readout pattern and electronics as one integrated, miniaturized, low power package utilizing a single substrate, and we are in the first phase of development of such a device. The readout will be constructed using multi-chip-module (MCM) PCB technology, widely used for low cost, robust, hybrid circuit manufacture. The Image Charge technique will be used to induce charge on a pattern of sense electrodes comprising an array of pads, each configured as a 50 Ω transmission line, impedance matched to individual channels of a high speed multi-channel preamplifier/discriminator ASIC. The ASIC dies will be mounted directly on the readout PCB in an MCM configuration. Interfacing to the outside world will be provided by an FPGA implemented digital controller. The entire readout /electronics package will be contained on a compact volume with a footprint comparable to the detector housing and interfacing to the outside world directly using a generic interface such as USB 2.0 or IEEE 1394.

The combination of Image Charge with an integrated readout and electronics component will enable us to build low mass, low power, robust readout devices of exceptional performance, with the ability to provide combinations of high spatial resolution, high temporal resolution, high events rates, and simultaneous event capability, depending on the choice of readout technology.

REFERENCES

1. C.D. Mackay, R.N. Tubbs, J.E. Baldwin, "Noise-Free Detectors in the Visible and Infrared: Implications for the Design of Next Generation AO Systems and Large Telescopes", Proc. SPIE, Vol. 4840, 2002, pp. 436-442

2. J.L.A Fordham, D.A. Bone, M.K. Oldfield, J.G. Bellis, T.J. Norton, "The MIC photon counting detector", Proceedings of an ESA Symposium on Photon Detectors for Space Instrumentation, 1994, pp 103.
3. C. Johnson, "Review of electron-bombarded CCD cameras", Proc. SPIE 3434, 1998, p. 45.
4. M. Lampton, F. Paresce, "The Ranicon: a resistive anode image converter", Rev. Sci. Instrum, 45(9), 1974, pp. 1098.
5. H.O. Anger, Instr.Soc.Am.Trans., 5, 1966, pp. 311.
6. O. Jagutzki, J. Barnstedt, U. Spillmann, L. Spielberger, V. Mergel, K. Ullmann-Pfleger, M. Grewing, and H. Schmidt-Bocking, "Fast-position and time-sensitive read-out of image intensifier for single photon detection", Proc. SPIE, 3764, 1999, pp. 61.
7. J.S. Lapington, "The effects of secondary electron emission on the operation of position sensitive anodes", Nucl. Instrum. Meth., vol. A392 (1997) p. 336.
8. J.S. Lapington, and H.E. Schwarz, "The design and manufacture of Wedge and Strip Anodes", IEEE Trans. Nucl. Sci., vol. NS-33 (1986) p. 288.
9. F. Anghinolfi, P. Jarron, F. Krummenacher, E. Usenko and M.C.S. Williams, "NINO, an ultra-fast, low-power, front-end amplifier discriminator for the Time-Of-Flight detector in ALICE experiment", IEEE Trans. Nucl. Sci., Vol. 51(5), 2004. pp. 1974 – 1978.
10. O. Jagutzki, J.S. Lapington, L.B.C.Worth, V. Mergel, H. Schmidt-Bocking, "Position sensitive anodes for MCP read-out via image charge detection", Nucl. Instr. Meth., A477, 2002, pp. 256